The EMBO Journal Vol.18 No.12 pp.3509–3519, 1999

Progressive *cis*-inhibition of telomerase upon telomere elongation

Stéphane Marcand[1,2,3], Vanessa Brevet[1] and Eric Gilson[1,4]

[1]Laboratoire de Biologie Moléculaire et Cellulaire, Ecole Normale Supérieure de Lyon, UMR8510 CNRS/ENSL, 69364 Lyon Cedex 07 and [2]Service de Biochimie et de Génétique Moléculaire, CEA/Saclay, 91191 Gif sur Yvette Cedex, France

[3]Permanent address: Service de Biochimie et de Génétique Moléculaire, CEA/Saclay, 91191 Gif sur Yvette Cedex, France

[4]Corresponding author
e-mail: Eric.Gilson@ens-lyon.fr

In yeast, the constant length of telomeric DNA results from a negative regulation of telomerase by the telomere itself. Here we follow the return to equilibrium of an abnormally shortened telomere. We observe that telomere elongation is restricted to a few base pairs per generation and that its rate decreases progressively with increasing telomere length. In contrast, in the absence of telomerase or in the presence of an over-elongated telomere, the degradation rate linked to the succession of generations appears to be constant, i.e. independent of telomere length. Together, these results indicate that telomerase is gradually inhibited at its site of action by the elongating telomere. The implications of this finding for the dynamics of telomere length regulation are discussed in this study.

Keywords: chromosome/flippase/telomerase/telomere/yeast

Introduction

Telomeres are essential to genome integrity and cell proliferation. They specifically cap the ends of linear chromosomes such that they are not recognized by DNA damage checkpoints and repair systems which would act on an accidental DNA break (Mc Clintock, 1941; Sandell and Zakian, 1993; van Steensel *et al*., 1998). They also allow the complete replication of chromosome ends, which cannot be accomplished by conventional DNA polymerases (Watson, 1972; Lingner *et al*., 1995). Furthermore, telomeres participate in several aspects of the functional organization of the whole nucleus, including transcriptional silencing (Gilson *et al*., 1993a; Marcand *et al*., 1996a).

In most organisms, such as yeast and vertebrates, the sequence of telomeric DNA consists of a tandem array of short guanine-rich repeats (Zakian, 1995). It is an oriented structure with the G-rich strand running 5′ to 3′ towards the distal end of the chromosome, and ending as a short single-stranded 3′ overhang. The length of this DNA varies according to species, cell type, chromosome end and age. In *Saccharomyces cerevisiae*, for example, the length of $TG_{1\text{-}3}$ telomeric repeats is kept within a narrow size distribution around a mean value of a few hundred base pairs (Shampay *et al*., 1984; Walmsley and Petes, 1985). The telomeric repeats are synthesized by a unique ribonucleo-protein reverse transcriptase called telomerase, which specifically extends the 3′ G-rich telomeric strand (reviewed in Nakamura and Cech, 1998; Nugent and Lundblad, 1998). The synthesis of the complementary 5′ C-rich telomeric strand seems most likely to be driven by the DNA polymerase α–primase complex (Price, 1997).

The telomeric chromatin can be divided into two distinct structural domains, both assuming the functions of chromosome capping and telomere length regulation. One domain is composed of a 3′ extension of the G-rich strand telomeric DNA or G tail, complexed with specific proteins (Virta-Pearlman *et al*., 1996; Labranche *et al*., 1998; Nugent *et al*., 1998). The second domain corresponds to the double-stranded telomeric repeats, and appears to be organized, at least in part, in a non-nucleosomal manner (Wright *et al*., 1992; Tommerup *et al*., 1994), and contains specific telomeric factors which play a critical role in telomere maintenance (reviewed in Brun *et al*., 1997). In *S.cerevisiae*, the double-stranded part of the $TG_{1\text{-}3}$ telomeric repeats is complexed to an array of Rap1p molecules, a telomeric DNA-binding factor (Conrad *et al*., 1990; Lustig *et al*., 1990; Klein *et al*., 1992; Wright *et al*., 1992; Gilson *et al*., 1993b). Similarly, in the fission yeast *Schizosaccharomyces pombe*, $TTAC(A)G_{2\text{-}5}$ telomeric repeats appear to interact with Taz1p (Cooper *et al*., 1997), and in humans, the double-stranded TTAGGG repeats are bound by TRF1 and TRF2 (Chong *et al*., 1995; Bilaud *et al*., 1996, 1997; Broccoli *et al*., 1997).

In several organisms, the telomere length of telomerase-positive cells is maintained at a constant mean value. This stability can be viewed as a balance between elongation and shortening (Larson *et al*., 1987; Greider, 1996). In *S.cerevisiae*, this equilibrium is determined by a negative regulation of telomerase activity by the telomere itself when its length exceeds a threshold value (Murray *et al*., 1988; Kyrion *et al*., 1992). This negative feedback appears to be mediated by a protein-counting mechanism that can discriminate the precise number of Rap1p molecules bound to a telomere (Kyrion *et al*., 1992; Brun *et al*., 1997; Marcand *et al*., 1997; Ray and Runge, 1999).

Several lines of evidence suggest that the *cis*-inhibition of telomerase by an excess of structural telomere components is a widespread mechanism used to regulate telomere length. In another budding yeast, *Kluyveromyces lactis*, Rap1p also negatively regulates telomere length, presumably by *cis*-inhibition of telomerase (McEachern and Blackburn, 1995; Krauskopf and Blackburn, 1996, 1998). In fission yeast, a deletion of *taz1* dramatically increases telomere length (Cooper *et al*., 1997; Nakamura *et al*., 1998). Similarly, in human cells a loss of function of TRF1 results in a significant telomere elongation

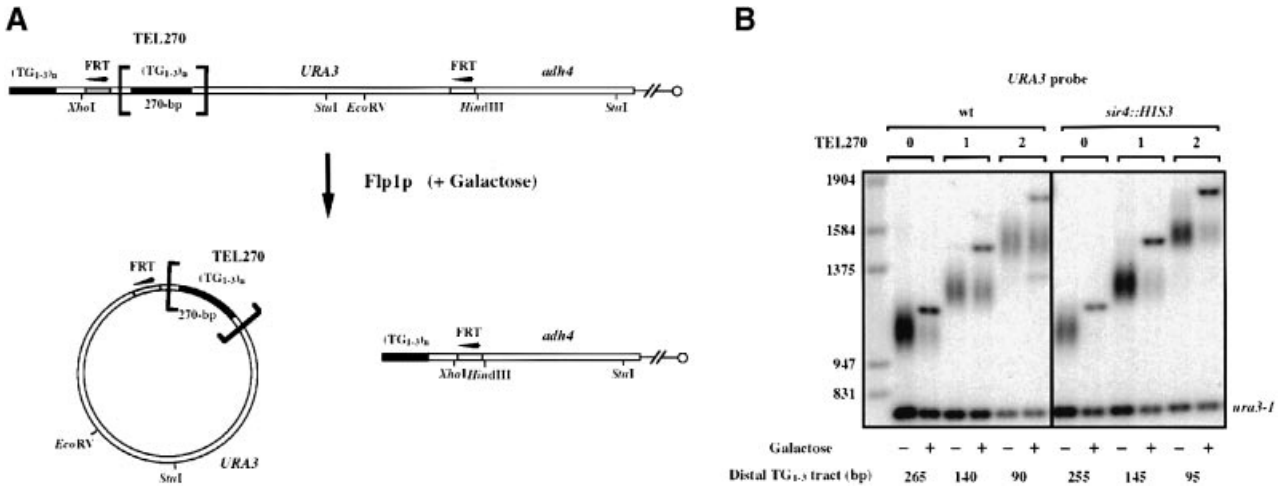

Fig. 1. Deletion of internal telomeric repeats and formation of an abnormally shortened telomere by an *in vivo* recombination event. (**A**) Schematic representation of the experimental system used in this study. The positions of the *Stu*I, *Eco*RV and *Xho*I restriction sites are indicated. The orientations of the telomeric repeats are represented by multiple arrowheads. (**B**) Yeast strains Lev187 (wt, no insert), Lev189 (wt, one TEL270 insert), Lev 220 (wt, two TEL270 inserts), Lev206 (*sir4::HIS3*, no insert), Lev207 (*sir4::HIS3*, one TEL270 insert) and Lev224 (*sir4::HIS3*, two TEL270 inserts) were grown in raffinose-containing medium (–) and exposed to 2% galactose for 4 h (+). Genomic DNAs were digested with *Eco*RV and *Hin*dIII, separated by electrophoresis on 0.9% agarose gel and blotted onto a nitrocellulose membrane. The membrane was probed with a 750 bp *Eco*RV–*Hin*dIII *URA3* fragment. The median length of the telomeric restriction fragment was measured with Image-Quant, using the non-telomeric, 750-bp *ura3-1* fragment as an internal control for each lane; 795 bp (no insert), 1100 bp (with one TEL270 insert) or 1405 bp (with two TEL270 inserts) was subtracted from this value to give the indicated size of the distal $TG_{1\text{-}3}$ tract.

(van Steensel and de Lange, 1997). Finally, ciliate telomere DNA-binding proteins are able to inhibit telomerase activity *in vitro* (Froelich-Ammon *et al*., 1998).

So far, telomere length regulation has been studied mainly at the steady-state level and the underlying dynamics behind the regulated length are still largely unknown. In this study, we investigated whether elongation arrest occurs suddenly when the telomere reaches its regulated length, or results from a gradual inactivation upon telomere elongation. For this purpose, we designed a new method to measure telomere elongation rate by following the return to equilibrium of an artificially shortened telomere in *S.cerevisiae*. We show that the rate of elongation decreases with increasing telomere length, revealing a progressive *cis*-inhibition of telomerase upon elongation.

Results

Experimental design

In order to follow the elongation of a telomere in yeast cells, we designed a system allowing us to reduce the size of a single telomere without affecting the integrity of its end. It has been shown previously that an internal telomeric tract of $TG_{1\text{-}3}$ repeats in the immediate vicinity of a telomere is taken into account by the length regulation mechanism (Marcand *et al*., 1997; Ray and Runge, 1999). Located between two specific sites for an inducible recombinase, such an internal telomeric tract could be deleted by an *in vivo* recombination event, leaving an abnormally short telomere in a wild-type context.

Specifically, the left extremity of chromosome VII beyond the *ADH4* gene was replaced by a short stretch of $(TG_{1\text{-}3})_n$ sequence and a *URA3* marker gene flanked by two Flp1p-recognition target (FRT) sites in direct repeat. Upon integration into the yeast genome, the short telomeric sequence serves as a 'seed' to build a new telomere (Gottschling *et al*., 1990; Lustig *et al*., 1990; Lustig, 1992; Singer and Gottschling, 1994), whose length is maintained at a constant mean value [~265 base pairs (bp) in strain Lev187 grown in raffinose-containing media]. One 320 bp fragment containing a block of 270 bp of telomeric repeats was inserted between the *URA3* gene and the telomere-proximal FRT site (Figure 1A). As shown in Figure 1B, this insert increases the mean size of the *Eco*RV telomeric restriction fragment by 205 bp, indicating that the mean size of the distal repeats is reduced from 265 to 140 bp. Thus, as expected, despite being separated from the very end of the chromosome by a linker sequence of 135 bp, the internal telomeric repeats are partially counted by the length-sensing mechanism. When a second 270 bp block of $TG_{1\text{-}3}$ repeats is added, the size of the distal repeats is reduced further to 90 bp (Figure 1B). The addition of a third block of $TG_{1\text{-}3}$ repeats does not significantly reduce further the size of the distal tract (data not shown).

Conditional expression of *FLP1* was obtained from an integrated copy of *GAL10-FLP1*, which is inactive when cells are grown in the absence of galactose but rapidly inducible following transfer to a galactose-containing medium (Holmes and Broach, 1996). As shown in Figure 1B, Flp1p induction converts the telomeric *URA3* gene into a circular molecule, visualized as a discrete band above the telomeric smear. Upon serial subculturing of the induced cells, the circular molecule disappeared and no additional fragment appeared by hybridizing an *Eco*RV genomic blot with a *URA3* probe (data not shown). This indicates that the circular recombination products are progressively lost from the cells, presumably by dilution due to their inability to initiate replication.

The recombination efficiency can be estimated by the amount of the circular form and/or by the relative disappearance of the parental telomeric smear. Interestingly, this efficiency appears to be reduced in the presence of internal telomere repeats (Figure 1B). The same experi-

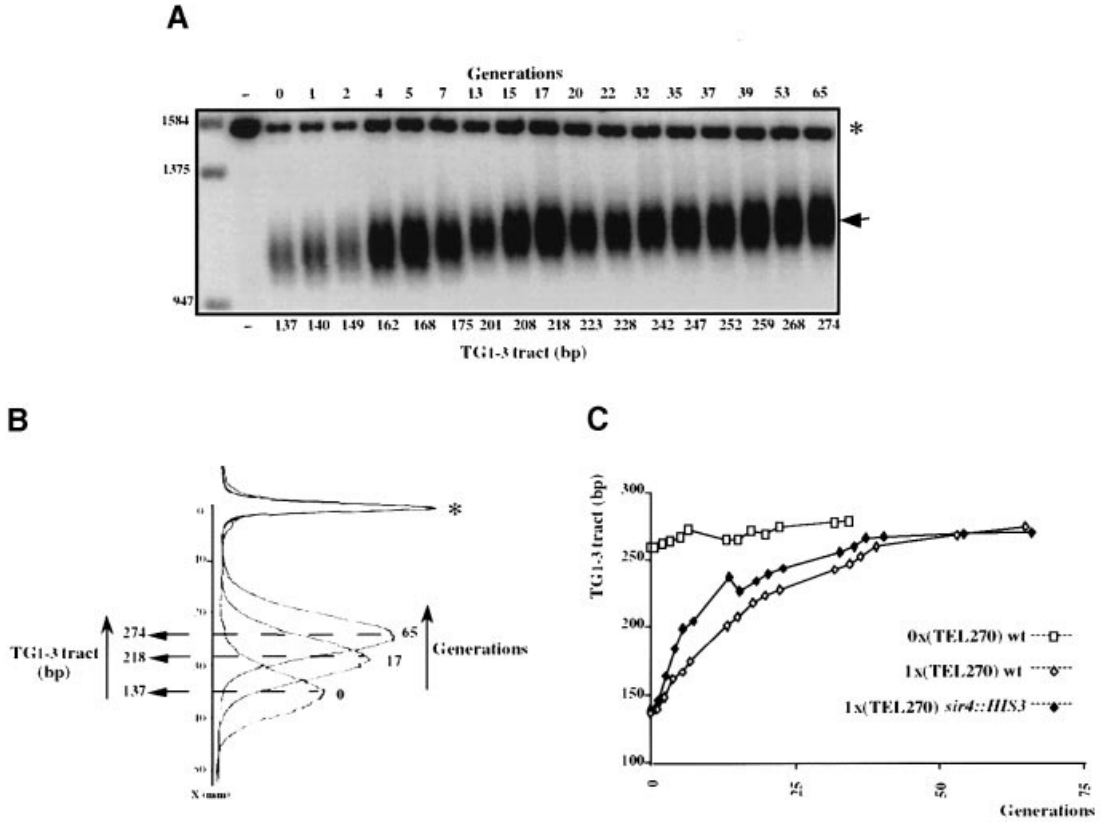

Fig. 2. Elongation kinetics of a shortened telomere in exponentially growing cells. Yeast strains were grown in raffinose-containing medium (–) and exposed to 2% galactose for 3 h (generation 0). Cell were resuspended in glucose-containing medium (YPD) and maintained in exponential growth for 4 days. The number of generations after induction was evaluated from cultural OD_{600}. Genomic DNA was digested with *Stu*I, separated by electrophoresis on 0.9% agarose gels and blotted onto a nitrocellulose membrane. The membrane was probed with an 840-bp *Hin*dIII–*Stu*I *ADH4* fragment. The median length of the telomeric restriction fragment was measured with Image-Quant, using the residual uninduced non-telomeric 1.56-kb *Stu*I *URA3-ADH4* fragment as an internal control for each lane [marked by an asterisk in (A) and (B)]. 929 bp were subtracted from this value to give the size of the TG_{1-3} tract. (**A**) Telomere elongation in yeast strain Lev189 (wild type, one TEL270 insert). The arrow indicates the telomeric restriction fragment. On the left, the size markers of 947, 1375 and 1584 bp are indicated. (**B**) Three examples of phosphoimaging scans of the hybridization signals in lanes corresponding to generations 0, 17 and 68 of the gel presented in (A). The dotted lines indicate the position of the apex of the telomere length profile. The *x*-axis represents the distance in millimeters between the uninduced 1.56-kb *Stu*I *URA3-ADH4* internal control and the apex. The *y*-axis represents the phosphor counts in arbitrary units. (**C**) Graphic representation of telomere elongation in yeast strains Lev187 (wild type, no insert, □), Lev189 (wild type, one TEL270 insert, ◇) and Lev207 (*Δsir4*, one TEL270 insert, ◆).

ments were repeated in isogenic strains in which the *SIR4* gene has been interrupted, causing a complete loss of transcriptional silencing at telomeres (Aparicio *et al*., 1991; data not shown). In this context, the recombination efficiency appears to increase (Figure 1B; data not shown), suggesting that the FRT sites are more accessible to the Flp1p recombinase in the absence of silencing, or alternatively that the silenced chromatin may sequester the circular molecule, favoring its reintegration into the VII-L telomere.

Kinetics of telomere elongation in exponentially growing cells

We followed the evolution of an abnormally shortened telomere in populations of exponentially growing cells over >60 generations. In this experiment, cells growing exponentially in raffinose were exposed to galactose for 3 h, during which time Flp1p was expressed and one to two divisions occurred. Cells were then washed, resuspended in glucose-containing rich medium and regularly diluted to maintain an exponential growth (OD_{600} <2). Aliquots were taken for genomic DNA extraction at various intervals and the length of the TG_{1-3} repeats was followed using the *ADH4* probe.

The elongation time courses starting from a mean length of ~260 bp and ~140 bp are displayed in Figure 2. In Figure 3, we show the results of two independent experiments starting from ~100 bp. Strikingly, telomere elongation took place progressively with successive generations and the steady-state length was reached after >50 generations. During elongation, the symmetrical distribution of telomere length, as revealed by phosphoimager scanning of Southern blots, does not seem to be altered (Figure 2B). This indicates that all the shortened telomeres are elongated in a coordinated manner. It can be seen that the control strain with an initial telomere length of ~260 bp displayed a slight but significant increase of ~15 bp (Figure 2C). This elongation seems to be due to the shift from raffinose- to glucose-containing media that occurs during the course of the experiment (data not shown). Such a slight modification of telomere length upon a change in carbon source has been reported previously by Sandell *et al*. (1994). Telomere elongation was also followed in strains with the *sir4* mutant allele. As shown in Figures 2 and 3, the kinetics of elongation in wild-type and mutant strains were indistinguishable within the limits of experimental errors. It is worth noting that this particular insertion mutant allele of *sir4* does not significantly reduce

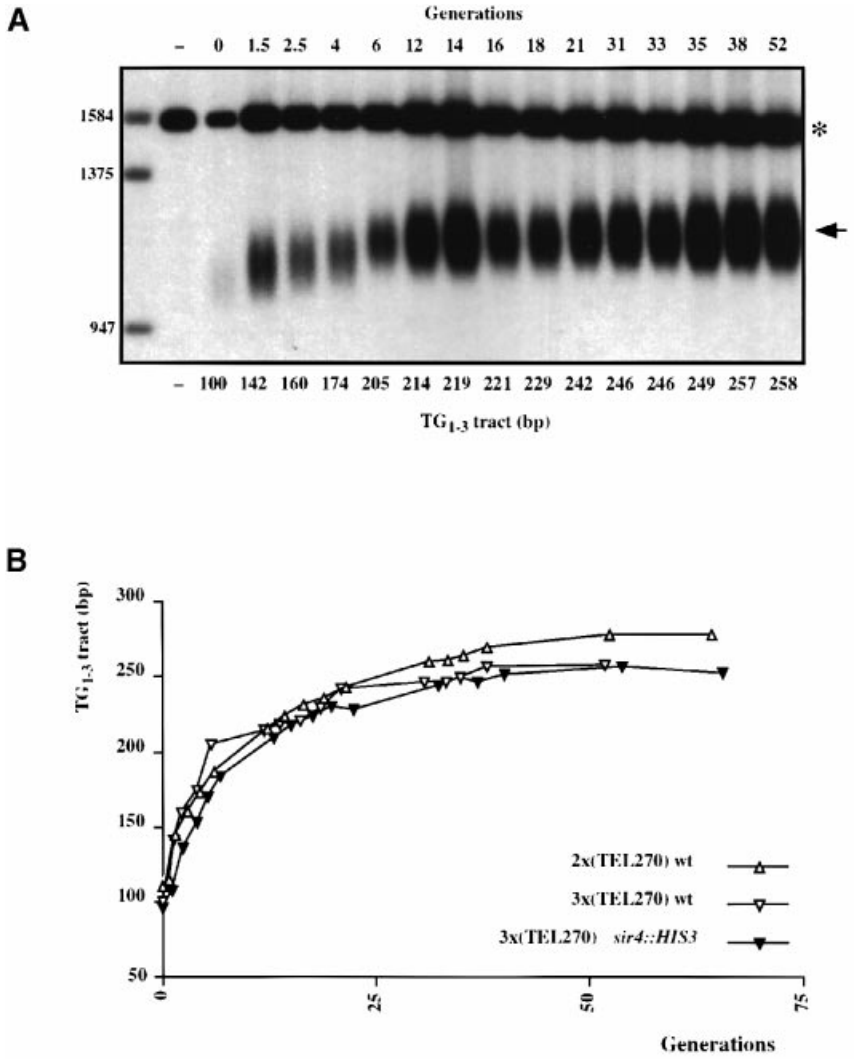

Fig. 3. (**A**) Telomere elongation in yeast strain Lev222 (wild type, three TEL270 inserts). The arrow and asterisk indicate the telomeric restriction fragment and the residual uninduced non-telomeric *URA3-ADH4* fragment, respectively. The mean telomere length was obtained as described in Figure 2. On the left, the size markers of 947, 1375 and 1584 bp are indicated. (**B**) Graphical representation of telomere elongation in yeast strains Lev220 (wild type, two TEL270 inserts, △), Lev222 (wild type, three TEL270 inserts, ▽) and Lev226 (*Δsir4*, three TEL270 inserts, ▼).

telomere length as other mutant alleles do (Palladino *et al*., 1993; Kennedy *et al*., 1995; data not shown).

As the telomere increases in size, the pace of telomere elongation seems to decrease rapidly. In order to get a more quantitative evaluation of the elongation rate at different lengths, we pooled the results of the experiments described previously. An approximation of the elongation rate was obtained by dividing the difference in telomere length between two successive experimental points by the corresponding number of generations. We then grouped these values according to their median telomere length in 20 bp ensembles. The median elongation rate for each of these ensembles is displayed graphically in Figure 4. A progressive reduction of the elongation rate with increasing telomere length is clearly visible, from ~15 bp/generation at the initial length of 140 bp, to <1 bp/generation in the immediate vicinity of the regulated length. In the *sir4* mutant, the evolution of the elongation rate appears very similar to that in the wild type; the slight variations between the two histograms are within the limits of the experimental errors (Figure 4).

Telomere elongation in Δrad50 and Δrad52 mutants

We then tested the elongation of an abnormally shortened telomere in two mutants that differentially affect telomere length regulation. A deletion of the *RAD50* gene severely reduces telomere length but does not further increase the growth defects due to a complete loss of telomerase activity, indicating that the *Δrad50* mutation partially affects the telomerase pathway (Nugent *et al*., 1998). In contrast, a deletion of the *RAD52* gene does not affect telomere length in the presence of telomerase (Dunn *et al*., 1984). However, in the absence of telomerase, the product of the *RAD52* gene is required for elongation of extremely short telomeres by an alternative pathway, probably based on unequal exchanges (Lendvay *et al*., 1996; McEachern and Blackburn, 1996).

Compared with wild type, the deletion of *RAD52* does not significantly reduce the length of the distal repeats after induction of Flp1p recombinase, and the shortened telomere appears to be elongated at a similar rate (Figure 5). In *Δrad50* cells containing two blocks of internal

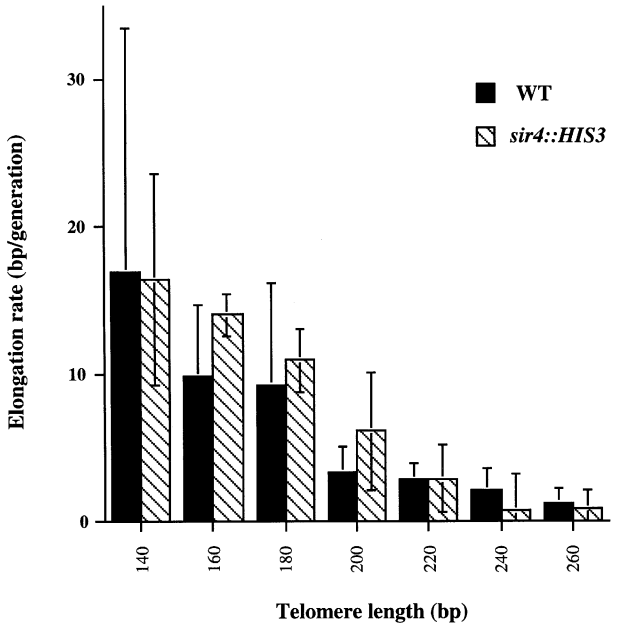

Fig. 4. Elongation rate according to telomere length. These median values are derived from the experiments described in Figures 2 and 3. The results from the wild-type strains Lev189, Lev220 and Lev222, and from the *sir4::HIS3* mutant strains Lev207 and Lev226, were pooled in two distinct groups. An approximation of the elongation rate was obtained dividing the difference in telomere length between two successive experimental points by the corresponding number of generations. These values are grouped according to their median telomere length in 20 bp ensembles. The median elongation rate and corresponding standard deviation for each of these ensembles are shown.

telomere repeats, the length of the distal repeats is reduced to ~50 bp after induction of the Flp1p recombinase (Figure 5). This very short telomeric tract obtained after induction was expected due to the reduced steady-state telomeric length in *Δrad50* cells as compared with wild type. Interestingly, the shortened telomere reaches a new equilibrium at a rate significantly slower than in *RAD50* cells, even for telomeres of a similar size (Figure 5).

Degradation rate in cells lacking telomerase activity

In the absence of telomerase, telomere length progressively decreases at an estimated rate of ~3- to 5-bp per generation (Singer and Gottschling, 1994; Lendvay *et al*., 1996; Nugent *et al*., 1996; Lingner *et al*., 1997). To quantify precisely the rate of shortening, we knocked out the *TLC1* gene encoding the RNA template of telomerase in a strain with an *URA3*-tagged telomere. Four independent *Δtlc1* clones were grown in rich medium and cells were diluted regularly to maintain exponential growth (OD_{600} <2). Aliquots were taken for genomic DNA extraction at various intervals and the length of the $TG_{1\text{-}3}$ repeats was followed using a *URA3* probe (Figure 6). At the beginning of the time course experiment (generation 0 in Figure 6), each individual clone contains *URA3*-tagged telomere of a different size.

As shown in Figure 6, telomere length decreases progressively over ~25 generations. Experimental points were relatively well aligned, allowing us to draw a linear regression curve for each independent experiment. For the four independent experiments, the slopes range from 2.7- to 3.1-bp/generation, with a mean at 2.95±0.2 bp/generation. Thus, the telomere shortening rate in the absence of telomerase appears to be constant within the range of telomere length used here.

Degradation rate of an over-elongated telomere

We next investigated the degradation rate when the telomerase is present but repressed *in cis* by an over-elongated telomere. Such telomeres introduced in wild-type strains are known to return to regulated length both by a progressive loss of telomeric tract and by stochastic single-step intrachromatid deletions (Kyrion *et al*., 1992; Li and Lustig, 1996). In order to obtain an accurate evaluation of the progressive degradation rate at different lengths, we followed the evolution of an over-elongated *URA3*-tagged telomere in wild-type strains over a large number of generations. A plasmid shuffle was used to replace the *rap1Δ670-807* allele, which results in the over-elongation of all telomeres, with the wild-type copy of *RAP1* (see Materials and methods). The presence of the wild-type *RAP1* gene product was checked by immunoblot analysis using antibodies against Rap1p. In all tested clones obtained after the shuffle, the wild-type form of Rap1p replaced the faster migrating form of the mutant protein (data not shown), and thus these clones contain over-elongated telomeres in a *RAP1* context.

As expected, serial liquid subculturing of independent *RAP1* clones containing an *URA3*-tagged VII-L telomere of ~600 bp revealed a progressive loss of telomeric DNA (Figure 7A and B). The shortening rate appears to be constant until telomere size approaches wild-type length. A slower shortening process then takes place to complete the return to equilibrium (Figure 7B). If a deletion of *EST1* is introduced after the shuffle, resulting in a complete loss of the telomerase pathway *in vivo* (Lendvay *et al*., 1996), no steady-state length is reached and shortening is pursued at a constant rate (Figure 7A and C). The rate of shortening is significantly higher in *Δest1* (~4 bp/generation) than in wild-type cells (~2 bp/generation) (Figure 7B and C). This raises the interesting possibility that a residual telomerase activity is still acting on the over-elongated telomere and/or that *EST1* can protect the telomere against degradation independent of its function in the telomerase complex. The latter hypothesis is also suggested by the fact that the degradation rate appears to be slightly higher in *Δest1* cells than in *Δtlc1* cells (Figures 6C and 7C).

The degradation pattern of *Δest1* cells appears to be the same in cells containing the *rap1-17* allele, a mutant form of Rap1p lacking the C-terminal part of the protein (Figure 7C), as in *RAP1* shuffled cells. This indicates that telomere over-elongation in *rap1-17* cells is *EST1*-dependent and that the shortening rate in the absence of *EST1* is independent of the C-terminus of Rap1p. In conclusion, in different genetic backgrounds, the rate of shortening appears to be a constant independent of telomere length.

Discussion

We present here an assay for measuring telomere elongation in yeast cells. Our method is based on an inducible shortening of a single telomere and a time course of the

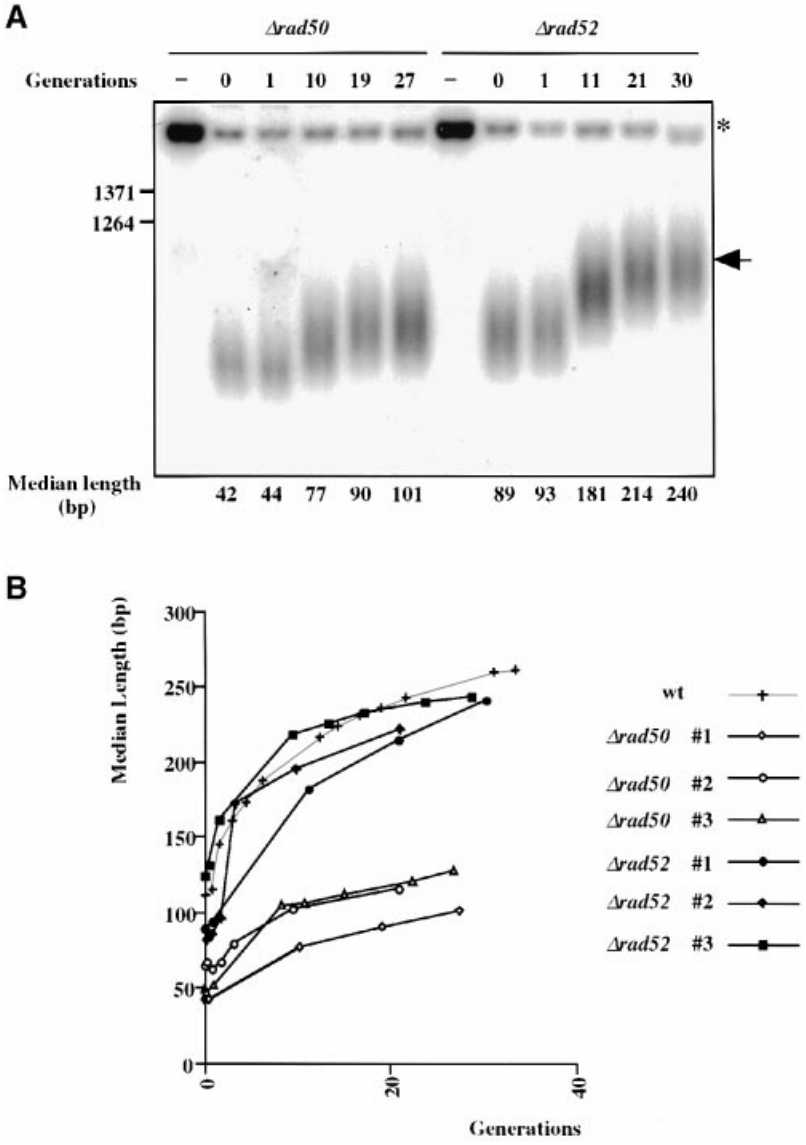

Fig. 5. (**A**) Telomere elongation in yeast strains Lev231 (*Δrad50*, two TEL270 inserts) and Lev232 (*Δrad52*, two TEL270 inserts). The arrow and asterisk indicate the telomeric restriction fragment and the residual uninduced non-telomeric *URA3-ADH4* fragment, respectively. The mean telomere length was obtained as described in Figure 2. Size markers are indicated on the left. (**B**) Graphic representation of telomere elongation in strains Lev231 (*Δrad50*, two TEL270 inserts) and Lev232 (*Δrad52*, two TEL270 inserts). Three independent experiments are displayed. The results from yeast strains Lev220 (wt, gray line) are reproduced from Figure 3.

evolution of the mean length. This system allows initiating telomere elongation on a template that can be as short as <100 nt, i.e. approximately one-third of the initial telomeric DNA length. Since the shortening occurs on the internal side of the telomere, the distal telomere structure is preserved throughout the experiment. Therefore, immediately after the induced shortening, the resulting telomere is expected to be competent for telomerase action.

Extremely short telomeres unable to carry out their essential protective function can be elongated by unequal exchanges, a pathway independent of telomerase but requiring the product of the *RAD52* gene (Lendvay *et al*., 1996; McEachern and Blackburn, 1996). In our assay, a deletion of the *RAD52* gene does not seem to modify the pattern of elongation rate (Figure 5), indicating that in the length range used here, Rad52p-dependent unequal exchanges are not responsible for the observed elongation. Hence, telomerase is most likely to be the only significant elongating activity in our assay. This was consistent with the decreasing elongation rate observed in cells disrupted for the *RAD50* gene (Figure 5), which appears to be involved in the telomerase-mediated pathway for telomere elongation (Nugent *et al*., 1998).

The rate of telomere elongation appears limited to a few base pairs per generation when cells are grown in exponential phase. During the return to equilibrium of an abnormally shortened telomere, the telomere elongation rate decreases progressively with increasing telomere length (Figure 4). The observed elongation rate is expected to be the outcome of the elongation by telomerase minus the progressive shortening process intrinsically linked to succession of the DNA replication cycles. Therefore, we measured the telomere shortening rate in two situations in which telomerase is inactivated, i.e. after disruption of *TLC1*, leading to the inactivation of the telomerase activity *in vitro* and *in vivo*, or of *EST1*, resulting in a loss of

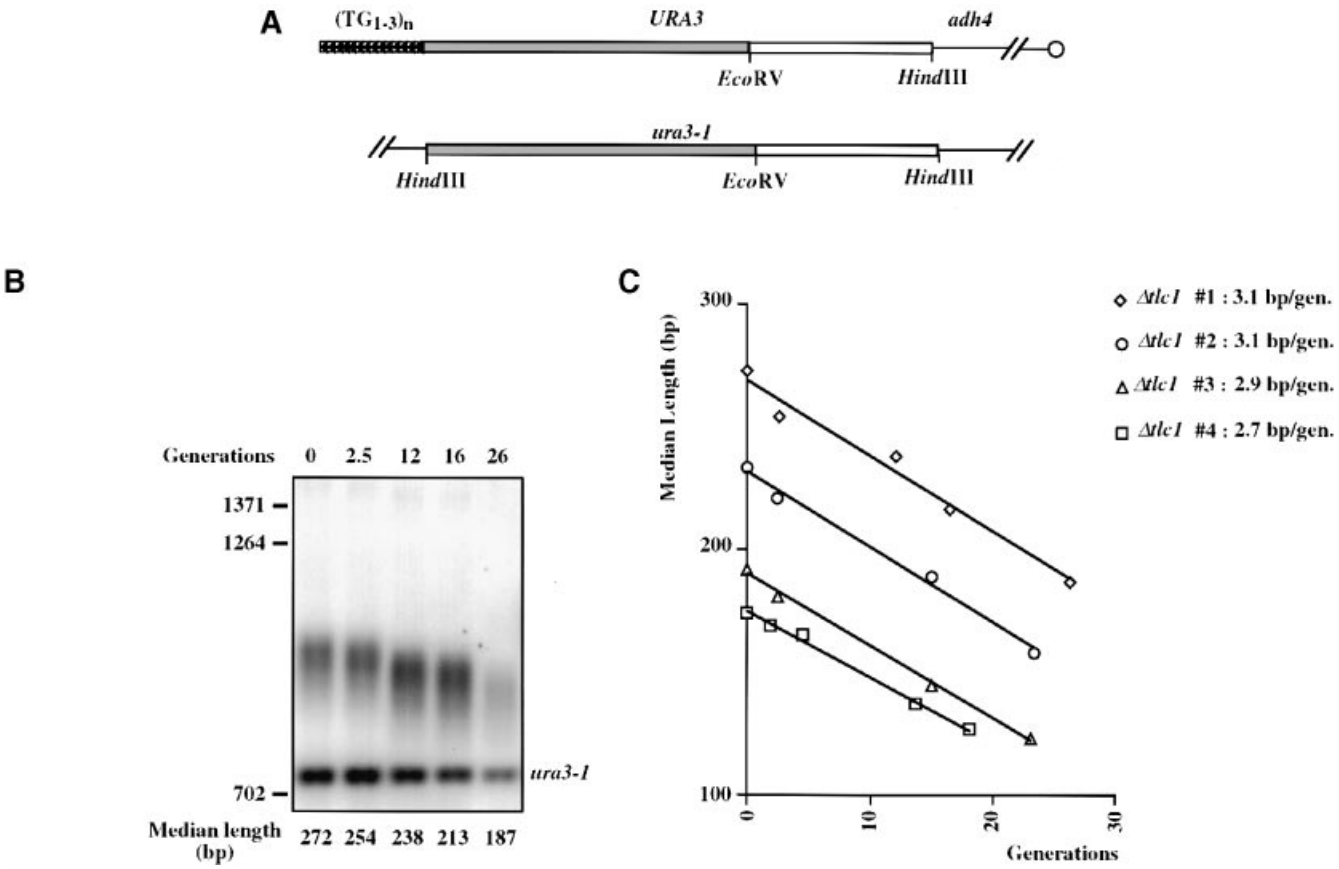

Fig. 6. Telomere shortening in absence of telomerase. (**A**) Schematic representation of the *URA3*-tagged telomere and of the *ura3-1* allele at its chromosomal location in strain Lev5. The positions of the *Eco*RV and *Hin*dIII restriction sites are indicated. The telomeric repeats are represented by multiple arrowheads. (**B**) The gene encoding the telomerase RNA template was deleted by homologous recombination in strain Lev5. Four independent *Δtlc1* clones were resuspended and grown exponentially in rich medium. Genomic DNAs were digested with *Eco*RV and *Hin*dIII, separated by electrophoresis on 0.9% agarose gel, and blotted onto a nitrocellulose membrane. The membrane was probed with a 757-bp *Eco*RV–*Hin*dIII *URA3* fragment. The median length of the telomeric restriction fragment was measured with Image-Quant, using the non-telomeric 757-bp *ura3-1* fragment as an internal control for each lane; 730 bp was subtracted from this value to give the indicated size of the $TG_{1\text{-}3}$ tract. On the left, the size markers of 702, 1264 and 1371 bp are indicated. (**C**) A graphic representation of four independent experiments. The one corresponding to the displayed blot is represented by diamonds. For each experiment, a linear regression curve has been drawn whose slope is indicated next to its respective symbol.

in vivo but not *in vitro* telomerase activity. In both cases, the shortening rate appears to be a constant independent of length, including the range of size corresponding to the elongation assay (Figures 6B and 7C). The constant degradation rates in the absence of telomerase allow us to conclude that the effective telomerase activity acting *in vivo* at an elongating telomere decreases progressively with increasing telomere length.

When telomerase is present but repressed at its site of action due to an over-elongated telomere, the telomere initially shortens at a constant pace with the successive generations. As it is approaching the vicinity of the regulated length, its pace of degradation progressively decreases and tends towards zero at equilibrium (Figure 7B). This progressive reduction in the 'apparent' degradation rate does not occur in absence of *EST1*. This indicates that the reduction is likely to be due to a progressive enhancement of telomerase activity near equilibrium and not to a reduction in the underlying shortening rate. In summary, in three different situations where the telomerase is genetically inactivated or *cis*-repressed, the degradation rate appears to be constant, independent of length.

Modeling telomere length equilibrium

To model the evolution of effective telomerase activity according to telomere length, we hypothesize that the elongation rate decreases with increasing length according to a linear function. A predicted time course based on this assumption is indistinguishable from the experimental data, as shown in Figure 8A. Therefore, although it is likely that the *in vivo* decline of telomere elongation obeys more complex functions, a linear model appears to be consistent with the *in vivo* behavior of an abnormally shortened telomere approaching the equilibrium in yeast.

In Figure 8B, efficient telomerase activity with respect to telomere length, viewed as a linear function and the shortening rate as a constant independent of length, is plotted. At equilibrium, the elongation and shortening rates are expected to balance, implying that the regulated length corresponds to the intersection between the two curves. This model provides a simple framework for explaining changes in telomere length caused by genetic modifications. First, it implies that telomere length at equilibrium will be sensitive to changes in the enzymatic properties of the telomerase. Indeed, in cells with specific

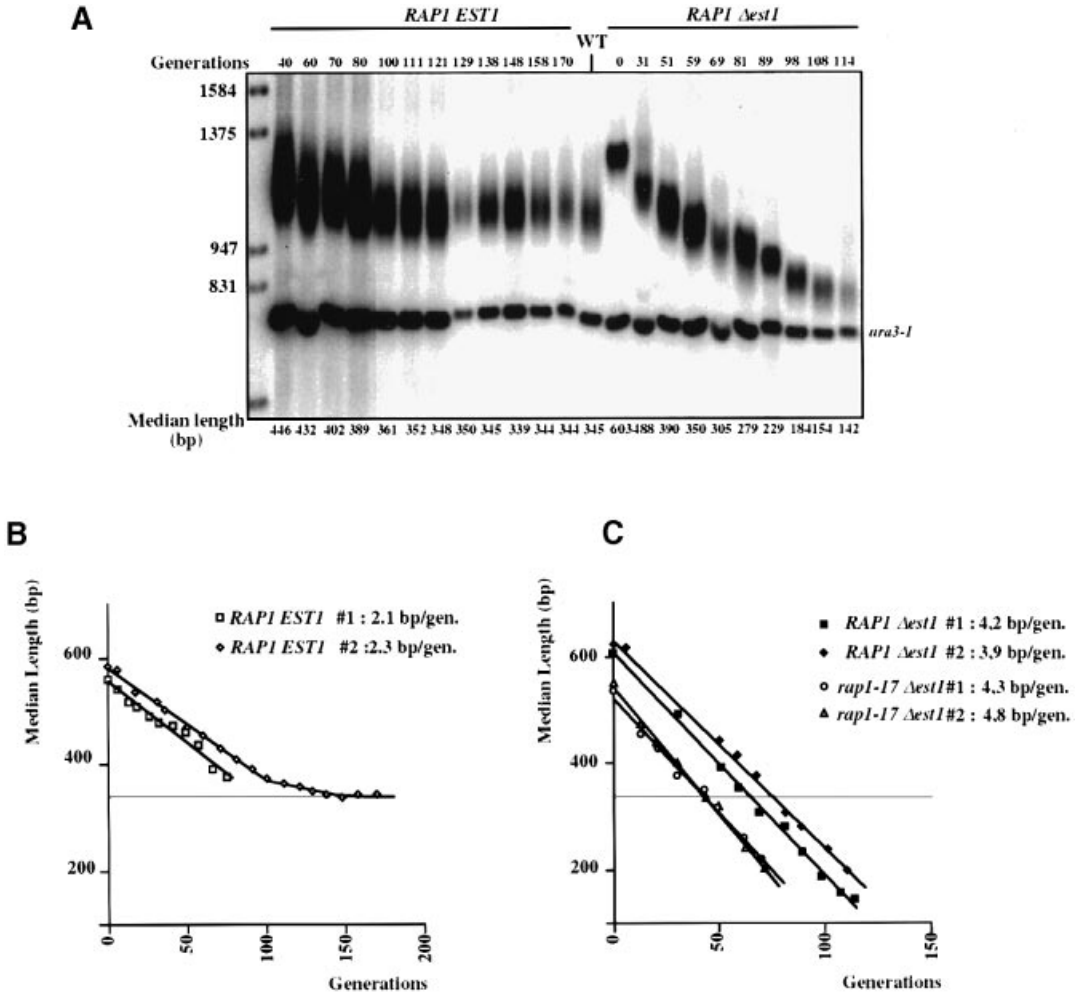

Fig. 7. Degradation of an over-elongated telomere. In wild-type cells, over-elongated telomeres were obtained by a shuffle replacing the *rap1Δ670-807* allele with the wild-type gene. In *RAP1 Δest1* cells, the *EST1* gene was deleted after the shuffle. In *rap1-17 Δest1* cells, the *EST1* gene was deleted in strain Lev135. (**A**) Growth conditions and determination of the mean telomere length of the *URA3*-tagged VII-L telomere are as described in Figure 6. On the left, the size markers of 831, 947, 1375 and 1584 bp are indicated. WT corresponds to a lane with DNA of wild-type cells with wild-type telomere length. (**B**) A graphic representation of two independent experiments using *EST1* cells. The one corresponding to the displayed blot, represented by diamonds, was followed for enough generations to reach the regulated wild-type length. For each experiment, a regression curve has been drawn for the linear portion of the curve. The corresponding slope is indicated next to its respective symbol. (**C**) A graphic representation of four independent experiments using either *RAP1 Δest1* cells or *rap1-17 Δest1* cells. The one corresponding to the blot in (A) is represented by filled squares. For each experiment, a linear regression curve has been drawn whose slope is indicated next to its respective symbol.

mutations in the template region of the telomerase RNA, a reduction of telomerase activity *in vitro* correlates with a reduction of the regulated telomere length and not with a total loss of telomeric DNA (Prescott and Blackburn, 1997). Similarly, point mutations in the reverse-transcriptase domain of the telomerase catalytic subunit can cause a decrease in telomere length, an effect probably due to a direct reduction in the enzymatic activity of telomerase (Lingner *et al*., 1997). This hypothesis is in agreement with our results showing that the elongation rate is reduced in *Δrad50* cells (Figure 5), which are believed to be partially deficient in the telomerase pathway (Nugent *et al*., 1998). Secondly, any increase of the shortening rate is predicted to cause a proportional decrease of telomere length. Interestingly, an important reduction of telomere length has been observed in cells lacking one of the Ku subunits, Hdf1p or Hdf2p (Boulton and Jackson, 1996; Porter *et al*., 1996). This length reduction correlates with an increase of the 3′ telomeric single-strand extension (Gravel *et al*., 1998), and the shortening rate is predicted to be directly linked to the mean size of this single-strand extension (Makarov *et al*., 1997). Furthermore, it has been shown that over-elongated telomeres decrease in size at a much higher rate in the absence of Hdf1p or Hdf2p (Polotnianka *et al*., 1998). Thus, it is tempting to suggest that the role of Hdf1p and Hdf2p in telomere length regulation at steady state can be explained, at least in part, by their impact on the degradation rate.

Mechanisms of telomerase cis-inhibition

The negative regulation of telomere elongation seems to be based on a mechanism discriminating the number of Rap1p molecules bound to the telomere (Marcand *et al*., 1997; Ray and Runge, 1999). In this work, we show that over-elongation due to lack of the Rap1p C-terminal domain is clearly dependent upon *EST1* (Figure 7C). This further indicates that telomerase is the target of the retro-inhibition of elongation due to an excess of Rap1p. We

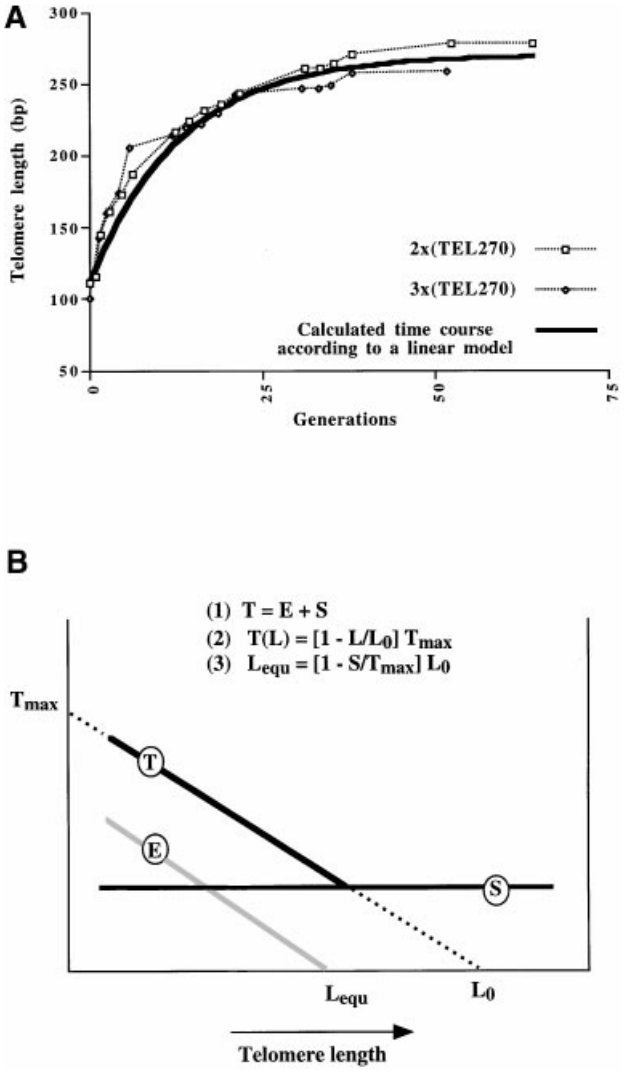

Fig. 8. (**A**) The calculated time course (thick line) was obtained as followed: the elongation rate (E), a linear function of telomere length (L), is described by the following equation (1): E (L) = [1 – L/L_{equ}] E_{max}; E_{max} is the extrapolated initial elongation rate when L = 0 and L_{equ} is the telomere length at the equilibrium. Using E_{max} = 20 bp/generation and L_{equ} = 270 bp, this equation becomes (2): E (L) = 20 – 0.074L. Telomere length, depending upon the succession of the generations (*n*), can be described by (3): L (*n*) = L (*n* – 1) + E [L (*n* – 1)]. Thus, L (*n*) = 0.926 L (*n* – 1) + 20. This equation was used to calculate a time course starting with L (0) = 110 bp. The results from yeast strains Lev220 (wild type, two TEL270 inserts, □) and Lev222 (wild type, three TEL270 inserts, ◇) are reproduced from Figure 3. (**B**) A model of telomere length regulation based on our measurement of the elongation rate of a shortened telomere (gray line marked by E) and of the degradation rate in the absence of telomerase (black line marked by S). The effective telomerase activity (black line marked by T) was deduced by making the sum of E and S, according to equation (1). S is a constant independent of telomere length. At each generation, T is an inverse linear function of telomere length (L) and is described by the equation (2). The two constants T_{max} and L_0 are the extrapolated initial telomerase activity and the telomere length sufficient to fully repress telomerase, respectively. Telomere length at the equilibrium (L_{equ}) is the length for which T = S and is described by equation (3).

propose that the gradual decline of telomerase activity reflects the cumulative effect of each individual Rap1p molecule assembled during elongation, up to a number of molecules (i.e. up to a length) sufficient to reduce telomerase activity *in cis* to a level precisely balancing the constant shortening rate. This mechanism of telomerase regulation acting at or near equilibrium is distinct from that mediated by intrachromatid recombination, which allows a rapid shortening of only a subset of over-elongated telomeres (Li and Lustig, 1996).

Two factors interacting with Rap1p, Rif1p and Rif2p, are required for telomere length regulation (Wotton and Shore, 1997), suggesting that the progressive inhibition of telomerase could be mediated by these proteins. At the molecular level, the action *in cis* of these proteins on the distally located telomerase is elusive. The progressive telomerase inhibition argues against a strong cooperative effect between them. Rather, it suggests the gradual folding of the telomere into a restrictive higher-order configuration that limits the number of bases that an individual telomerase can add during one generation and/or the probability that the enzyme acts on its substrate.

Interestingly, the fact that short telomeres are expected to be preferred substrates for telomerase was hypothesized on the basis of non-symmetrical length distribution of vertebrate telomeres (Lansdorp *et al*., 1996; Ducray *et al*., 1999). Furthermore, a progressive return to equilibrium of telomeres that were too short was reported previously in telomerase-positive animal cells (Barnett *et al*., 1993; Spung *et al*., 1999). Thus, the inverse relation between the effective telomerase activity and telomere length, as demonstrated in this work for budding yeast, may represent a general mechanism used in several organisms to avoid critical telomere shortening.

Materials and methods

Yeast strains

The yeast strains used in this study are all derivatives of W303-1A and are listed in Table I. All gene disruptions or replacements used to generate these strains were confirmed by Southern blot analysis. Plasmid pFV17, a *LEU2*-marked, integrating vector containing the *FLP1* gene controlled by the *GAL10* promoter (Volkert and Broach, 1986), was cut by *Bst*EII and integrated into the *leu2* locus in strain W303-1A to yield strain Lev172. Overexpression of the *FLP1* gene in strains bearing the endogenous 2μ plasmid is toxic (Reynolds *et al*., 1987); accordingly, cells lacking the endogenous 2μ plasmid were identified by plating strain Lev172 on galactose medium and recovering rare robust colonies. Strain Lev178 is one of such clones which was tested free of 2μ plasmid by Southern analysis.

Strains Lev205 results from the transformation of Lev178 with the linearized plasmid pJR276 (*sir4::HIS3*; Kimmerly and Rine, 1987). Strains Lev187, Lev189, Lev220 and Lev222 result from the transformation of Lev178 with the linearized plasmids sp225, sp228, sp242 and sp243, respectively. Strains Lev207, Lev224 and Lev226 result from the transformation of Lev205 with the linearized plasmids sp228 sp242 and sp243, respectively.

Strains Lev5 and Lev7 and plasmids sp17 and sp18 are described in Marcand *et al*. (1996b). A plasmid shuffle was used to generate the clones required to determine the degradation rate of an over-elongated telomere in wild type. Strain Lev7 carrying the chromosomal *rap1::LEU2* allele and the *rap1Δ670-807* mutant allele on the plasmid sp18 was transform with plasmid sp17 encoding the *RAP1* wild-type allele. The *EST1* gene was disrupted with the linearized plasmid *est-Δ1::HIS3* (Lundblad and Szotak, 1989). The *TLC1* gene was disrupted with the linearized plasmid pBlue61::LEU2 (Singer and Gottschling, 1994). The strain Lev135 was obtained from a cross between Lev5 and strain AJL440-1c bearing the *rap1-17* allele (Liu *et al*., 1994).

Plasmid DNAs

A first FRT site was inserted between the *URA3* and *adh4* sequences at the *Hin*dIII site of plasmid sp59 (Marcand *et al*., 1997), using oligonucleotides Flp*Hin*d#1 (5′-AGCTTCTGAAGTTCCTATACTTTC TAGAGAATAGGAACTTCGGAATAGGAACTTCAAGATCCCGGG-3′)

Table I. Yeast strains

Strain	Genotype
W303–1A	*MAT***a** *ade2-1 trp1-1 ura3-1 leu2-3,112 his3-11,15 can1-100*
Lev5	W303α *adh4::URA3-TEL*
Lev7	W303α *rap1::LEU2 adh4::URA3-TEL pRAP1-Sup4*
Lev135	W303α *rap1-17 adh4::URA3-TEL*
Lev172	W303a *leu2::LEU2-GAL10-FLP1 [cir+]*
Lev178	W303a *leu2::LEU2-GAL10-FLP1 [cir°]*
Lev205	Lev178 *sir4::HIS3*
Lev187	Lev178 *adh4::FRT-URA3-FRT-TEL*
Lev189	Lev178 *adh4::FRT-URA3-TEL270-FRT-TEL*
Lev220	Lev178 *adh4::FRT-URA3-TEL270-TEL270-FRT-TEL*
Lev222	Lev178 *adh4::FRT-URA3-TEL270-TEL270-TEL270-FRT-TEL*
Lev207	Lev205 *adh4::FRT-URA3-TEL270-FRT-TEL*
Lev224	Lev205 *adh4::FRT-URA3-TEL270-TEL270-FRT-TEL*
Lev226	Lev205 *adh4::FRT-URA3-TEL270-TEL270-TEL270-FRT-TEL*
Lev231	Lev220 *rad50::KAN*
Lev232	Lev220 *rad52::KAN*

and Flp*Hin*d#2 (5′-AGCTCCCGGGATCTTGAAGTTCCTATTCCG-AAGTTCCTATTCTCTAGAAAGTATAGGAACTTCAGA-3′), creating plasmid sp224 with a unique *Hin*dIII site distal of *URA3*. A second FRT site was inserted between the *URA3* gene and the 80-bp telomere repeat tract at the *Bam*HI site of sp224, using oligonucleotides FlpBmh#1 (5′-GATCCCTGAAGTTCCTATACTTTCTAGAGAATAGGAACTT-CGGAATAGGAACTTCAAGACTCGAGA-3′) and FlpBmh#2 (5′-GAT-CTCTCGAGTCTTGAAGTTCCTATTCCGAAGTTCCTATTCTCTAG-AA- AGTATAGAACTTCAGG-3′), creating plasmid sp225 with a unique *Bam*HI site distal of the telomere repeats. Plasmid sp229 (with a 270 bp telomere repeat tract) was created by inserting an *Eco*RI end-filled fragment from pLTel (Gilson *et al*., 1993b) into sp225 cut with *Bam*HI. Plasmid sp242 (with two 270 bp telomere repeat tracts) was created by inserting an *Eco*RI end-filled fragment from pLTel into sp229 cut with *Acc*65I. Plasmid sp243 (with three 270 bp telomere repeat tracts) was created by inserting an *Eco*RI end-filled fragment from pLTel into sp242 cut with *Acc*65I. Plasmids sp225, sp229, sp242 and sp243 were linearized with *Not*I and *Sal*I prior to transformation into yeast.

Southern blot analysis and telomere length measurement

Genomic DNAs were extracted with glass-bead/phenol-chloroform, digested with relevant restriction enzymes, separated by electrophoresis on 0.9% agarose gel, and blotted onto a nitrocellulose membrane. The membrane was probed with a radioactive probe labeled by random priming. Each blot was scanned using a Molecular Dynamics phospho-imager. With the Image-Quant software, a line was drawn down the middle of each lane, including the telomeric fragment and the non-telomeric fragment. Along this line, the signal was counted by adding the counts along an 8-mm orthogonal line. A graph was then drawn: the *x*-axis represented the distance from the bottom of the gel, and the *y*-axis represented the number of counts. Two peaks appeared; a sharp one (the non-telomeric fragment) and a smooth larger one (the telomeric fragment). The center of each peak was easily defined manually with a vertical line drawn by the computer, by moving with the mouse. The position of this line was given with 0.1 mm precision. The relative distance between the two fragments, therefore, was calculated very precisely, as the distance between the two was usually >3 cm. This value was then converted to a difference in bp using a semi-log equation whose slope was specific to the relative migration of the molecular weight markers on the gel. Analyzing the same gels by two different experimenters, or the same samples on two different gels, the actual error in telomere length measurements was estimated empirically to be <10 bp.

Acknowledgements

We would like to thank David Shore, James Broach, Daniel Gottschling and Victoria Lundblad for plasmids, Susan Gasser for Rap1p antibodies, and Scott Holmes for advice regarding the Flp1p system. We are grateful to Michel Charbonneau, Moira Cockell, Geneviève Fourel, Serge Gangloff, Nathalie Grandin, Joachim Lingner, Carl Mann and Marie-Claude Marsolier for advice and critical reading of the manuscript. S.M. is especially grateful to Carl Mann for supporting the completion of his work in his laboratory. This work was supported by the Association pour la Recherche contre le Cancer, the Ligue Nationale contre le Cancer, the Région Rhône-Alpes, the programme CNRS 'Génome' and the Association Française de Lutte contre la Mucovisidose (AFLM).

References

Aparicio,O.M., Billington,B.L. and Gottschling,D.E. (1991) Modifiers of position effect are shared between telomeric and silent mating-type loci in *S.cerevisiae*. *Cell*, **66**, 1279–1287.

Barnett,M.A., Buckle,V.J., Evans,E.P., Porter,A.C., Rout,D., Smith,A.G. and Brown,W.R. (1993) Telomere directed fragmentation of mammalian chromosomes. *Nucleic Acids Res.*, **21**, 27–36.

Bilaud,T., Koering,C.E., Binet-Brasselet,E., Ancelin,K., Pollice,A., Gasser,S.M. and Gilson,E. (1996) The telobox, a Myb-related telomeric DNA binding motif found in proteins from yeast, plants and human. *Nucleic Acids Res.*, **24**, 1294–1303.

Bilaud,T., Brun,C., Ancelin,K., Koering,C.E., Laroche,T. and Gilson,E. (1997) Telomeric localization of TRF2, a novel human telobox protein. *Nature Genet.*, **17**, 236–239.

Boulton,S.J. and Jackson,S. (1996) Identification of a *Saccharomyces cerevisiae* Ku80 homologue: roles in DNA double strand break rejoing and in telomeric maintenance. *Nucleic Acids Res.*, **24**, 4639–4648.

Broccoli,D., Smogorzewska,A., Chong,L. and de Lange,T. (1997) Human telomeres contain two distinct Myb-related proteins, TRF1 and TRF2. *Nature Genet.*, **17**, 231–235.

Brun,C., Marcand,S. and Gilson,E. (1997) Proteins that bind to double-stranded regions of telomeric DNA. *Trends Cell Biol.*, **7**, 317–324.

Chong,L., van Steensel,B., Broccoli,D., Erdjument-Bromage,H., Hanish,J., Tempst,P. and de Lange,T. (1995) A human telomeric protein. *Science*, **270**, 1663–1667.

Conrad,M.N., Wright,J.H., Wolf,A.J. and Zakian,V.A. (1990) RAP1 protein interacts with yeast telomeres *in vivo* : overproduction alters telomere structure and decreases chromosome stability. *Cell*, **63**, 739–750.

Cooper,J.P., Nimmo,E.R., Allshire,R.C. and Cech,T.R. (1997) Regulation of telomere length and function by a Myb-domain protein in fission yeast. *Nature*, **385**, 744–747.

Ducray,C., Pommier,J.P., Martins,L., Boussin,F. and Sabatier,L. (1999) Telomere dynamics, end-to-end fusions and telomerase activation during the human fibroblast immortalization process. *Oncogene*, in press.

Dunn,B., Szauter,P., Pardue,M.L. and Szostak,J.W. (1984) Tranfer of yeast telomeres to linear plasmids by recombination. *Cell*, **39**, 191–201.

Froelich-Ammon,S.J., Dickinson,B.A., Bevilacqua,J.M., Schultz,S.C. and Cech,T.R. (1998) Modulation of telomerase activity by telomere DNA-binding proteins in *Oxytricha*. *Genes Dev.*, **12**, 1504–1514.

Gilson,E., Laroche,T. and Gasser,S. (1993a) Telomeres and the functional architecture of the nucleus. *Trends Cell Biol.*, **3**, 128–134.

Gilson,E., Roberge,M., Giraldo,R., Rhodes,D. and Gasser,S.M. (1993b) Distortion of the DNA double helix by RAP1 at silencers and multiple telomeric binding sites. *J. Mol. Biol.*, **231**, 293–310.

Gottschling,D.E., Aparicio,O.M., Billington,B.L. and Zakian,V.A. (1990) Position effect at *S.cerevisiae* telomeres: reversible repression of PolII transcription. *Cell*, **63**, 751–762.

Gravel,S., Larrivee,M.P.L. and Wellinger,R.J. (1998) Yeast Ku as a regulator of chromosomal DNA end structure. *Science*, **280**, 741–744.

Greider,C.W. (1996) Telomere length regulation. *Annu. Rev. Biochem.*, **65**, 337–365.

Holmes,S.G. and Broach,J.R. (1996) Silencers are required for the inheritance of the repressed state in yeast. *Genes Dev.*, **10**, 1021–1032.

Kennedy,B.K., Austriaco,N.R.,Jr, Zhang,J. and Guarente,L. (1995) Mutation in the silencing gene SIR4 can delay aging in *S.cerevisiae*. *Cell*, **80**, 485–496.

Kimmerly,W. and Rine,J. (1987) Replication and segregation of plasmids containg *cis*-acting regulatory sites of silent mating type genes in *S.cerevisiae* are controlled by the *SIR* genes. *Mol. Cell. Biol.*, **7**, 4225–4237.

Klein,F., Laroche,T., Cardenas,M.E., Hofmann,J.F.X., Schweizer,D. and Gasser,S.M. (1992) Localization of RAP1 and topoisomerase II in nuclei and meiotic chromosomes of yeast. *J. Cell Biol.*, **117**, 935–948.

Krauskopf,A. and Blackburn,E.H. (1996) Control of telomere growth by interaction of RAP1 with the most distal telomeric repeats. *Nature*, **383**, 354–357.

Krauskopf,A. and Blackburn,E.H. (1998) Rap1 protein regulates telomere turnover in yeast. *Proc. Natl Acad. Sci. USA*, **95**, 12486–12491.

Kyrion,G., Boakye,K.A. and Lustig,A.J. (1992) C-terminal truncation of RAP1 results in the deregulation of telomere size, stability and function in *Saccharomyces cerevisiae*. *Mol. Cell. Biol.*, **12**, 5159–5173.

Labranche,H., Dupuis,S., Ben-David,Y., Bani,M.R., Wellinger,R.J. and Chabot,B. (1998) Telomere elongation by hnRNP A1 and a derivative that interacts with telomeric repeats and telomerase. *Nature Genet.*, **19**, 199–202.

Lansdorp,P.M., Verwoerd,N.P., van de Rijke,F.M., Dragowska,V., Little, M.T., Dirks,R.W., Raap,A.K. and Tanke,H.J. (1996) Heterogeneity in telomere length of human chromosomes. *Hum. Mol. Genet.*, **5**, 685–691.

Larson,D.D., Spangler,E.A. and Blackburn,E.H. (1987) Dynamics of telomere length variation in *Tetrahymena thermophila*. *Cell*, **50**, 477–483.

Lendvay,T.S., Morris,D.K., Sah,J., Balasubramanian,B. and Lundblad,V. (1996) Senescence mutants of *Sacharomyces cerevisiae* with a defect in telomere replication identify three additional *EST* genes. *Genetics*, **144**, 1399–1412.

Li,B. and Lustig,A.J. (1996) A novel mechanism for telomere size control in *S.cerevisiae*. *Genes Dev.*, **10**, 1310–1326.

Lingner,J., Cooper,J.P. and Cech,T.R. (1995) Telomerase and DNA end replication: no longer a lagging strand problem? *Science*, **269**, 1533–1534.

Lingner,J., Hughes,T.R., Shevchenko,A., Mann,M., Lunblad,V. and Cech,T.R. (1997) Reverse transcriptase motifs in the catalytic subunit of telomerase. *Science*, **276**, 561–567.

Liu,C., Mao,X. and Lustig,A.J. (1994) Mutational analysis defines a C-terminal tail domain of RAP1 essential for telomeric silencing in *S.cerevisiae*. *Genetics*, **138**, 1025–1040.

Lundblad,V. and Szotak,J.W. (1989) A mutant with a defect in telomere elongation leads to senescence in yeast. *Cell*, **57**, 633–643.

Lustig,A.J. (1992) Hoogsteen G–G base pairing is dispensable for telomere healing in yeast. *Nucleic Acids Res.*, **20**, 3021–3028.

Lustig,A.J., Kurtz,S. and Shore,D. (1990) Involvement of the silencer and UAS binding protein RAP1 in regulation of telomere length. *Science*, **250**, 549–553.

Makarov,V.L., Hirose,Y. and Langmore,J.P. (1997) Long G tails at both ends of human chromosomes suggest a C strand degradation mechanism for telomere shortening. *Cell*, **88**, 657–666.

Marcand,S., Gasser,M.S. and Gilson,E. (1996a) A sticky silence. *Curr. Biol.*, **6**, 1222–1225.

Marcand,S., Bucks,S.W., Moretti,P., Gilson,E. and Shore,D. (1996b) Silencing of genes at nontelomeric sites in yeast is controlled by sequestration of silencing factors at telomeres by Rap 1 protein. *Genes Dev.*, **10**, 1297–1309.

Marcand,S., Gilson,E. and Shore,D. (1997) A protein-counting mechanism for telomere length regulation in yeast. *Science*, **275**, 986–990.

Mc Clintock,B. (1941) The stability of broken ends of chromosomes in *Zea mays*. *Genetics*, **26**, 234–282.

McEachern,M.J. and Blackburn,E.H. (1995) Runaway telomere elongation caused by telomerase RNA gene mutations. *Nature*, **376**, 403–409.

McEachern,M.J. and Blackburn,E.H. (1996) Cap-prevented recombination between terminal telomeric repeat arrays (telomere CPR) maintains telomeres in *Kluyveromyces lactis* lacking telomerase. *Genes Dev.*, **10**, 1822–1834.

Murray,A.W., Claus,T.E. and Szostak,J.W. (1988) Characterization of two telomeric DNA processing reactions in *Saccharomyces cerevisiae*. *Mol. Cell. Biol.*, **8**, 4642–4650.

Nakamura,T.M. and Cech,T.R. (1998) Reversing time: origin of telomerase. *Cell*, **92**, 587–590.

Nakamura,T.M., Cooper,J.P. and Cech,T.R. (1998) Two modes of survival of fission yeast without telomerase. *Science*, **282**, 493–496.

Nugent,C.I. and Lundblad,V. (1998) The telomerase reverse transcriptase: components and regulation. *Genes Dev.*, **12**, 1073–1085.

Nugent,C.I., Hughes,T.R., Lue,N.F. and Lundblad,V. (1996) Cdc13p: a single-strand telomeric DNA-binding protein with a dual role in yeast telomere maintenance. *Science*, **274**, 249–252.

Nugent,C.I., Bosco,G., Ross,L.O., Evans,S.K., Salinger,A.P., Moore,J.K., Haber,J.E. and Lundblad,V. (1998) Telomere maintenance is dependent on activities required for end repair of double-strand breaks. *Curr. Biol.*, **8**, 657–660.

Palladino,F., Laroche,T., Gilson,E., Pillus,L. and Gasser,S.M. (1993) The positioning of yeast telomeres depends on SIR3, SIR4 and the integrity of the nuclear membrane. *Cold Spring Harbor Symp. Quant. Biol.*, **58**, 733–746.

Polotnianka,R.M., Li,J. and Lustig,A.J. (1998) The yeast Ku heterodimer is essential for protection of the telomere against nucleolytic and recombinational activites. *Curr. Biol.*, **8**, 831–834.

Porter,S.E., Greenwell,P.W., Ritchie,K.B. and Petes,T.D. (1996) The DNA-binding protein Hdf1p (a putative Ku homologue) is required for maintening normal telomere length in *S.cerevisiae*. *Nucleic Acids Res.*, **24**, 582–585.

Prescott,J. and Blackburn,E.H. (1997) Telomerase RNA mutations in *Sacchoromyces cerevisiae* alter telomerase action and reveal nonprocessivity *in vivo* and *in vitro*. *Genes Dev.*, **11**, 528–540.

Price,C.M. (1997) Synthesis of the telomeric C-strand. A review. *Biokhimiya*, **62**, 1216–1223.

Ray,A. and Runge,K.W. (1999) The yeast telomere length counting machinery is sensitive to sequences at the telomere-nontelomere junction. *Mol. Cell. Biol.*, **19**, 31–45.

Reynolds,A.E., Murray,A.W. and Szostak,J.W. (1987) Roles of the 2 μm gene products in stable maintenance of the 2 μm plasmid of *Saccharomyces cerevisiae*. *Mol. Cell. Biol.*, **7**, 3566–3573.

Sandell,L.L. and Zakian,V.A. (1993) Loss of a yeast telomere: arrest, recovery and chromosome loss. *Cell*, **75**, 729–739.

Sandell,L.L., Gottschling,D.E. and Zakian,V.A. (1994) Transcription of a yeast telomere alleviates telomere position effect without affecting chromosome stability. *Proc. Natl Acad. Sci. USA*, **91**, 12061–12065.

Shampay,J., Szostak,J.W. and Blackburn,E.H. (1984) DNA sequences of telomeres maintained in yeast. *Nature*, **310**, 154–157.

Singer,M.S. and Gottschling,D.E. (1994) *TLC1*: template RNA component of *Saccharomyces cerevisiae* telomerase. *Science*, **266**, 404–409.

Spung,C.N., Reynolds,G.E., Jasin,R. and Murnane,J.P. (1999) Chromosome healing in mouse embryonic stem cells. *Proc. Natl Acad. Sci. USA*, in press.

Tommerup,H., Dousmanis,A. and de Lange,T. (1994) Unusual chromatin in human telomeres. *Mol. Cell. Biol.*, **14**, 5777–5785.

van Steensel,B. and de Lange,T. (1997) Control of telomere length by the human telomeric protein TRF1. *Nature*, **385**, 740–743.

van Steensel,B., Smogorzewska,A. and de Lange,T. (1998) TRF2 protects human telomeres from end-to-end fusions. *Cell*, **92**, 401–413.

Virta-Pearlman,V., Morris,D.K. and Lundblad,V. (1996) Est1 has the properties of a single-stranded telomere end-binding protein. *Genes Dev.*, **10**, 3094–3104.

Volkert,F.C. and Broach,J.R. (1986) Site-specific recombination promotes plasmid amplification in yeast. *Cell*, **46**, 541–550.

Walmsley,R.M. and Petes,T.D. (1985) Genetic control of chromosome length in yeast. *Proc. Natl Acad. Sci. USA*, **82**, 506–510.

Watson,J.D. (1972) Origin of concatemeric DNA. *Nature New Biol.*, **239**, 197–201.

Wotton,D. and Shore,D. (1997) A novel Rap1p-interacting factor, Rif2p, cooperates with Rif1p to regulate telomere length in *Saccharomyces cerevisiae*. *Genes Dev.*, **15**, 748–760.

Wright,J.H., Gottschling,D.E. and Zakian,V.A. (1992) *Saccharomyces* telomeres assume a non-nucleosomal chromatin structure. *Genes Dev.*, **6**, 197–210.

Zakian,V.A. (1995) Telomeres: beginning to understand the end. *Science*, **270**, 1601–1607.

Received February 15, 1999; revised and accepted April 27, 1999